NJC

PAPER

View Article Online
View Journal | View Issue

Cite this: *New J. Chem.*, 2016, **40**, 4588

A sensitive AIEE probe for amphiphilic compounds†

Veerabhadraiah Palakollu,[a] Anuji K. Vasu,[a] Vijay Thiruvenkatam[b] and Sriram Kanvah*[a]

Received (in Montpellier, France) 10th September 2015,
Accepted 9th March 2016

DOI: 10.1039/c5nj02398j

www.rsc.org/njc

α-Cyanostilbene substituted with dimethylaniline and hydroxyl groups exhibits profound intensity enhanced bathochromic shifts in an aqueous medium as compared to organic solvents. These conspicuous emission changes are attributed to aggregation as a consequence of restricted intramolecular rotation. This observation is commonly termed as aggregation induced enhanced emission (AIEE). Single crystal X-ray crystallographic data suggest a zigzag molecular packing arrangement with intermolecular hydrogen bonding between –CN and –OH moieties. This unique observation is exploited as a diagnostic tool to probe amphiphilic compounds in aqueous media. Fluorescence investigations reveal that at lower surfactant concentrations emission due to aggregation is preserved, while at higher surfactant concentrations the aggregated emission is lost with concomitant changes to the micelle structure. Dynamic light scattering (DLS) and Scanning Electron Microscopy (SEM) experiments were used to examine the effect of surfactants on the particle size and morphology, respectively. This sensitive AIEE fluorescence response can also be visually observed by using a hand-held UV lamp.

Introduction

Suitably substituted fluorophores with fascinating aggregation induced enhanced emission (AIEE)[1] characteristics have attracted tremendous attention as promising materials for optoelectronic applications.[2–4] In the past decade, realizing their importance, a number of such fluorogens (metalloles,[5] tetraphenylethenes,[6,7] triphenylethenes,[8] distyrylanthracenes,[9] distyrylbenzenes,[10,11] α-cyanostilbenes[12–14] and other similar AIEE active materials[15,16]) have been established for a variety of applications. In contrast to weak or no fluorescence in the solution state, the AIEE fluorogens have greater emissive properties in the aggregated state. The enhanced emission in these systems is due to the restriction of intramolecular and intermolecular interactions, conformational planarization,[17] *cis–trans* isomerization,[10] crystal packing, or a combination of these factors.[1] In effect, this restriction of rotation enables radiative decay leading to a strong emission behavior[18–20] of the fluorophore. This phenomenon found a variety of applications such as organic light emitting diodes (OLEDs), chemical sensors for volatile organic compounds,[1,21] detectors of cyanides,[22] detectors of explosives, biological applications,[2,23–25] *etc.* Many of these applications draw strength from the intense fluorescence signal detected in the fluorophores in their aggregated state. This intense fluorescence signal due to AIEE can overcome the non-radiative decay processes that typically limit the utilization of many fluorophores for sensing applications. In this report, we demonstrate the use of this conspicuous signal of stilbene (**1**) in aqueous media as a 'beacon' for amphiphilic compounds such as surfactants. Stilbene (**1**) contains a donor group (dimethylamino group), an acceptor (cyano group) and a hydroxyl group. The acceptor is located on the unsaturated double bond while the dimethylamine and hydroxyl groups are located *para* to each other at opposite ends of the aromatic framework separated by a vinylic bond [Scheme 1]. The hydroxyl group may be used as a synthetic handle to expand the fluorescent framework and the presence of donor and acceptor groups helps in conservation of charge transfer. These results reveal remarkable utility of stilbene (**1**) as a fluorescence probe for surfactants in determining their critical micelle concentration and for visual detection.

Experimental section

Materials, methods and instruments

All the chemicals, reagents and surfactants (CTAB, SDS, Triton-X 100) used in this study were purchased from Aldrich, Alfa Aesar, Acros and S. D. Fine. The UV-Vis absorption spectra were recorded using an Analytik Jena Specord 210 plus spectrophotometer and the fluorescence emission studies were performed using a Horiba-Jobin Yvon Fluolorog-3 spectrofluorometer with a slit-width

[a] *Department of Chemistry, Indian Institute of Technology Gandhinagar, Indian Institute of Technology Gandhinagar, Ahmedabad-382424, India. E-mail: kanvah@gatech.edu*
[b] *Department of Biological Engineering, Indian Institute of Technology Gandhinagar, Ahmedabad 382424, India. E-mail: vijay@iitgn.ac.in*

† Electronic supplementary information (ESI) available: Tables S1 and S2 and Fig. S1–S7 are provided. CCDC 1031951. For ESI and crystallographic data in CIF or other electronic format see DOI: 10.1039/c5nj02398j

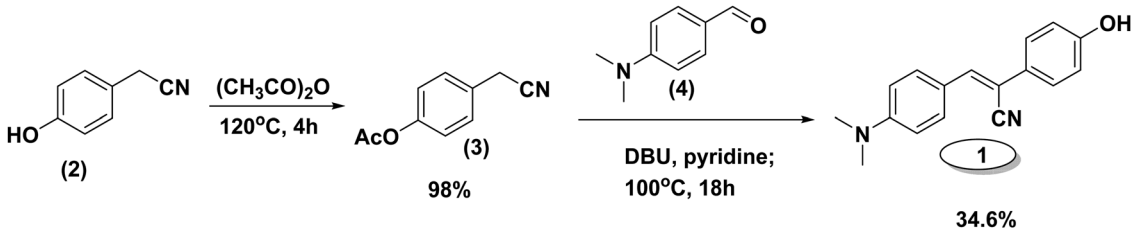

Scheme 1 Schematic of synthesis of stilbene (**1**) investigated.

of 1 or 2 nm at an excitation wavelength of 390 nm. Particle sizes were analyzed using a Nicomp 380 ZLS Zeta potential/particle sizer. Scanning electron microscopy (SEM) analysis was carried out using field emission SEM (JSM 7600F JEOL). For this purpose, one drop of the sample [$\sim 10^{-5}$ M aqueous solution of (**1**) – same solution that was used for fluorescence studies] was deposited on a silicon wafer mounted on an aluminum stub with the help of a double-sided adhesive carbon tape. The samples were heat dried at 45 °C for 12 hours and vacuum dried for 30 minutes to ensure complete removal of any residual water and coated with platinum before being analyzed. For the determination of the critical micelle concentrations (CMCs), 20 μL volumes of stock solution of the dye (1×10^{-4} M) in dioxane were added to different concentrations of surfactant solutions (1 mL). Fluorescence life-times were determined by using an Edinburgh Lifespec II instrument with a 375 nm excitation source, and recorded the emission decay profiles at 5 different wavelengths. Ludox HS-40 colloidal silica (40 wt% suspension in water) was used to record the instrument response function (IRF). The error associated with the lifetime fitting is in the range of 1.1–2.1%.

Synthesis of stilbene

The α-cyanostilbene as shown in Scheme 1 was synthesized *via* a simple condensation reaction and reported elsewhere.[26]

X-ray crystallographic details

Crystallographic data for the compound (*Z*)-3-(4-(dimethylamino)-phenyl)-2-(4-hydroxyphenyl)acrylonitrile were collected on a SuperNova (Dual, Cu source at zero) diffractometer with an EOS detector. The crystal data were collected at room temperature (293 K). The reflection data were integrated and reduced using Olex2,[27] Superflip.[28] The crystal structure was refined and solved using the WinGX suite (Version 2014.1)[27] & Ortep-3.[29] The crystal structures were solved by direct methods using SHELXS97[30] and refined by the full matrix least-squares method using SHELXL97 present in the program suite WinGX. The ORTEP diagrams of the compound were generated using ORTEP-3 and the packing diagrams were generated using Mercury.[31] Geometrical calculations were carried out using PARST[32] and PLATON.[33] All the hydrogen atoms associated with the carbon, oxygen and nitrogen atoms were fixed in geometrically constrained positions and refined isotropically. Fluorescence microscopy images were recorded by using a Zeiss AXIO observer A1 inverted microscope. A drop of the dye surfactant solution was kept on a clean glass slide and a cover slip was kept on top of the drop. Images were recorded using a FITC filter. Fluorescence intensities of the spots were measured by using the imageJ software by averaging about 50–70 spots.

Results and discussion

Fluorescence response of (1) and aggregation

Dimethylamino α-cyanostilbene (**1**) was prepared *via* the previously reported procedure. Stilbene (**1**) exhibits a weak emission behavior in homogeneous organic solvents but shows a significant bathochromic shift with a concomitant intensity enhancement in water (Fig. S1, ESI†). This observation is attributed to the AIEE phenomenon.[4,26] To clearly reveal the formation of the aggregates, scanning electron microscopy (SEM) of the sample of (**1**) in distilled water was carried out and the image reveals the formation of random aggregate like structures [Fig. 1]

To get molecular level information, single crystals were obtained by slow evaporation from an acetone/dioxane (6 : 4) solvent mixture at room temperature. Table S1 (ESI†) summarizes the crystal data of stilbene (**1**) and Fig. 2a depicts the ORTEP diagram with the numbering schemes and the packing interactions. As shown in Table S1 (ESI†), stilbene (**1**) crystallizes in the orthorhombic crystal system [CCDC 1031951] with a distinctive zigzag molecular packing arrangement (Fig. 2b). In addition, there are two molecules in the asymmetric unit cell and eight molecules in a symmetric unit cell. The tilt or the torsion angle associated with the central atoms, C7–C8–C9–C10, is 156.08° and that of C19–C8–C9–C14 is 157.17°, which assist in the O–H···N hydrogen bonding interactions. These O–H···N hydrogen bonds are separated by a distance of 2.04 Å and they allow the interaction of two neighboring molecules. The donor and acceptor units are separated by a dihedral

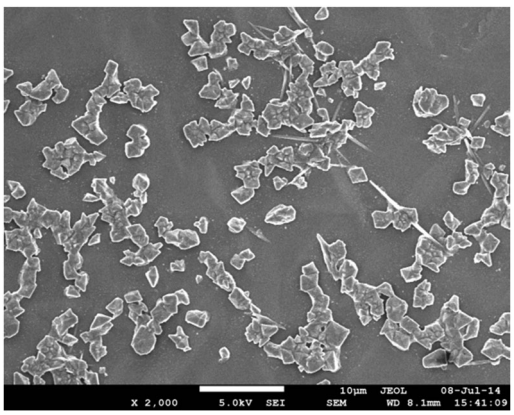

Fig. 1 SEM micrograph of stilbene (**1**) in distilled water (scale: 10 μm).

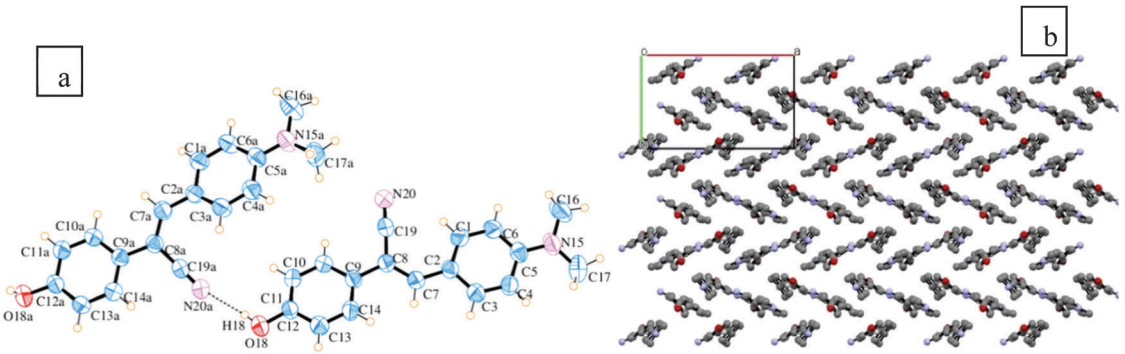

Fig. 2 (a) ORTEP diagram with 50% probability ellipsoids. The dotted lines indicate intermolecular contacts. (b) The unit of packing diagram with mercury CSD.[34]

angle of 163.4 and they support strong intermolecular hydrogen bonding interactions. This H-bonding interaction stabilizes the zig-zag or criss-cross packing arrangements. Other packing details and structural parameters are given in the ESI† [Fig. S2 and Table S1].

Fluorescence response of (1) in surfactants

Surfactant molecules and micelle solutions play an important role in many areas involving chemistry, biology and pharmaceutical applications.[35] Several methods were utilized to determine the CMC of the surfactants[36,37] but most established spectrophotometric methods are based on intensity changes of the fluorophores. Achieving a clear shift in emission with changes in the micellar structure yields an excellent spectroscopic signal to determine the CMC of the surfactants.[38] As a demonstration of this, we have chosen cetyltrimethylammonium bromide (CTAB), sodium dodecyl sulfate (SDS) and polyoxyethylene octyl phenyl ether (Triton X-100)

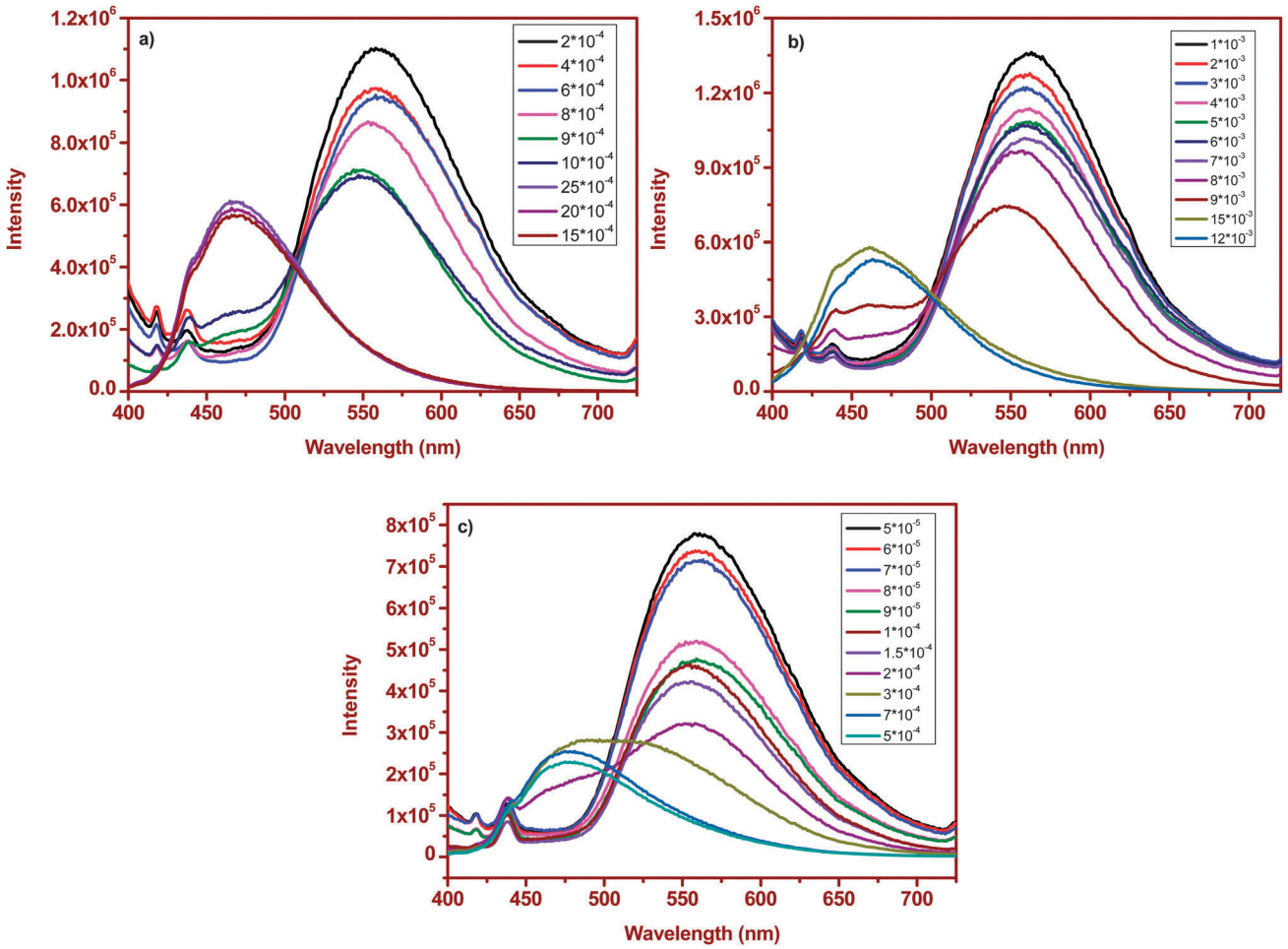

Fig. 3 Emission spectral changes of stilbene (**1**) with varying surfactant concentrations: (a) CTAB, (b) SDS and (c) Triton X-100.

as cationic, anionic and neutral surfactants. The absorption spectrum of (**1**) in surfactant solutions is given in Fig. S3 (ESI†). Fluorophore (**1**) absorbs at ~396 nm in water and no significant changes were observed upon interaction with the surfactant. However, we noticed distinct changes in the emission response. Fluorophore (**1**) emits at ~550 nm in distilled water. At lower concentrations (below CMC) of the surfactant, (**1**) emits at ~550 nm, similar to that observed in distilled water. This correlation of emission behavior in water and micellar environments indicates that the emission is likely due to the aggregated species. SEM images, shown below, confirm the similarity in the observed aggregation pattern. As the concentration of the surfactant is increased, a small hypsochromic shift in emission with a decrease in the intensity is observed. But as soon as the surfactant concentration approaches the CMC, the emission is strongly blue-shifted and a dominant emission at ~460–475 nm [Fig. 3a–c] was observed. This blue-shifted emission maximum is comparable to that observed in non-polar dioxane. Based on these comparable emission data, we can attribute the localization of the molecule to the non-polar regions of the micelle that contains hydrophobic chains. A further increase in concentration maintains the emission intensity or wavelength. Thus, at higher surfactant concentrations, where the fluorophore is localized in the hydrophobic micellar regions, the AIEE properties are lost, and at lower surfactant concentrations, the AIEE properties are seen with emission similar to that observed in water. As the molecule moves away from water towards the interior of the micelle, the aggregation pattern of the stilbene is also disturbed [Fig. 4b], leading to dispersal of particles of different sizes in comparison to that observed at lower surfactant concentrations [Fig. 4a]. The SEM images of (**1**) in CTAB, SDS and Triton-X 100 at above and below the CMC are shown in Fig. 4, and the image patterns demarcate the morphology of the aggregates formed. The CMCs of the surfactants calculated via a plot of intensity change (either at ~560 nm or at ~460–475 nm) *versus* concentration of the surfactant [Fig. 5 and Table 1] show good correlation with that reported in the literature.[39]

Visually detecting this emission response via possible color changes will have a better impact compared to the utilization of an instrumental response. As shown in Fig. 6 (and Fig. S3, ESI†), the addition of micromolar quantities of (**1**) reveals distinguishing colors

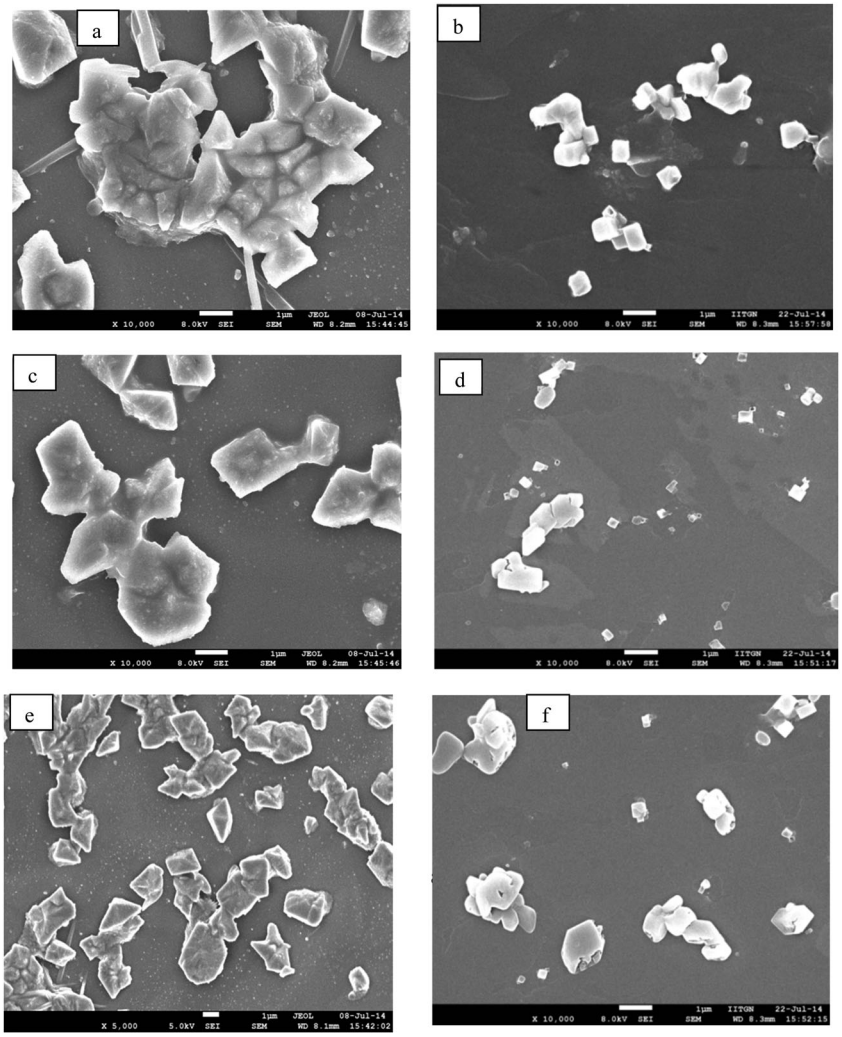

Fig. 4 SEM images of stilbene (**1**) in CTAB: (a) 2×10^{-4} and (b) 15×10^{-4}; in SDS: (c) 1×10^{-3} M and (d) 15×10^{-3} M; and in Triton X-100: (e) 5×10^{-5} M and (f) 7×10^{-4} M (scale: 1 μm).

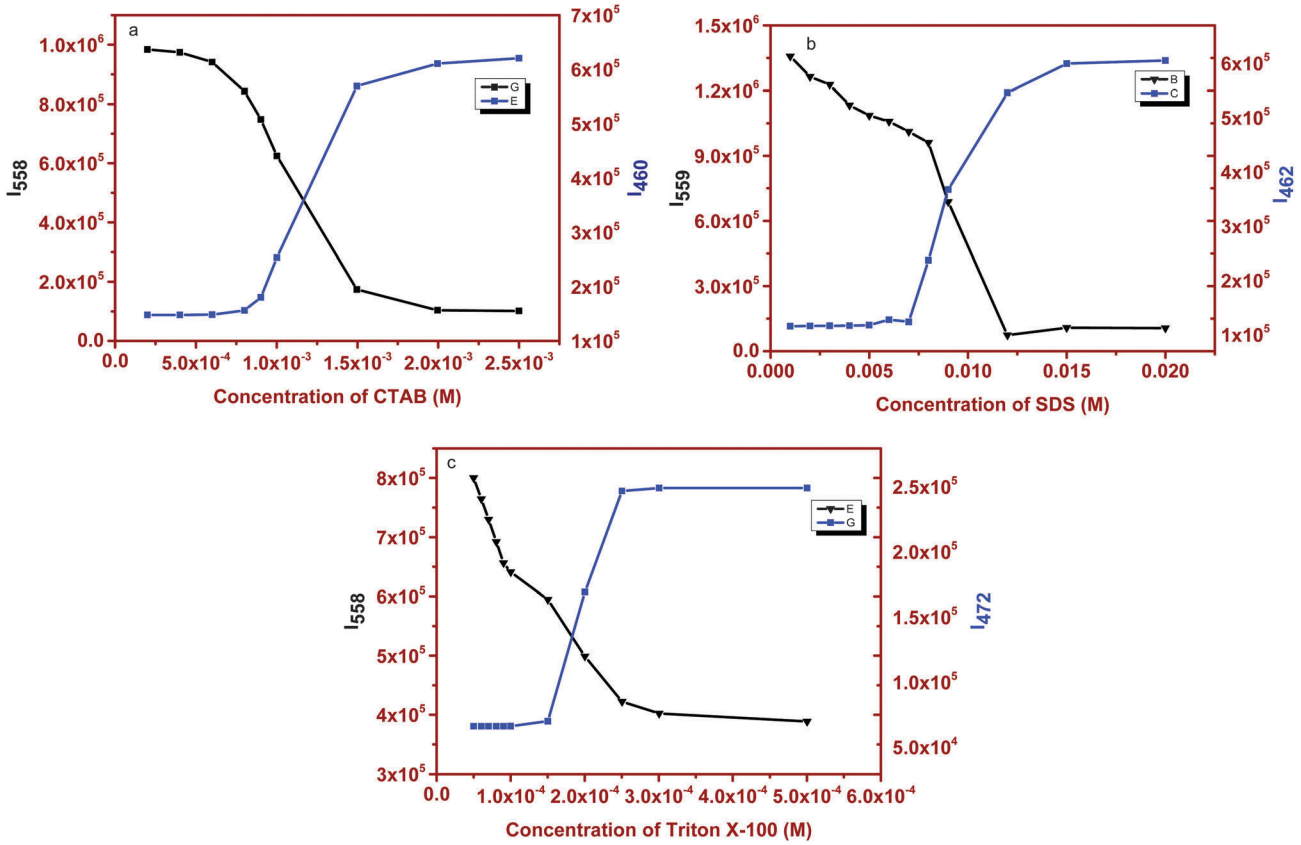

Fig. 5 Fluorescence emission spectral changes of stilbene (**1**) as a function of concentration of (a) CTAB, (b) SDS and (c) Triton X-100.

Table 1 CMC values of the surfactants

Surfactant	Calculated CMC (mM)	Literature values
SDS	8.8	7.5–9.1
Triton X-100	0.22	0.17–0.30
CTAB	1.01	0.80–1.04

(two colors) at above and below the critical micelle concentration of the surfactants. These color changes are distinguishable only when micelle formation occurs (Fig. S4, ESI†). For instance, in CTAB, stilbene (**1**) shows a fluorescent green color and correspondingly emits at ~550 nm at a lower surfactant concentration. As the concentration is increased, this greenish solution changes to a pale greenish-blue shade with a clear shift in the emission wavelength (~460 nm). The colors are fairly uniform at other concentrations of the surfactant. A similar behavior is noted for SDS and Triton X-100 with different color shades. This dual-color observance offers an easier identification in predicting the formation of the micelle.

Fluorescence microscope image analysis of the probe in different surfactant concentrations reveals [Fig. S5, ESI†] changes in the fluorescence intensity of the probe (measured using the imageJ software). These observations correlate with our previous emission spectral data.

Effects of surfactants on the aggregation of α-cyanostilbene

Apart from the changes in the emission wavelength, we examined the effects of change in surfactant concentration on the aggregation behavior of α-cyanostilbene. The particle size analysis of the fluorophore in water and surfactants was carried out using DLS to understand the changes in the sizes of aggregates and is shown in Fig. 7 and Fig. S6 (ESI†). The size distribution of the

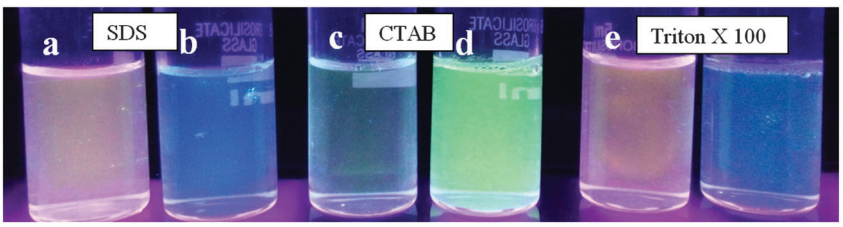

Fig. 6 Visual colors of stilbene (**1**) (2×10^{-5} M) at different concentrations of surfactants. (a & b) SDS at 2×10^{-3} M & 9×10^{-3} M; (c & d) CTAB at 0.4×10^{-3} M & 2×10^{-3} M; and (e & f) Triton X-100 at 0.05×10^{-3} M & 0.5×10^{-3} M.

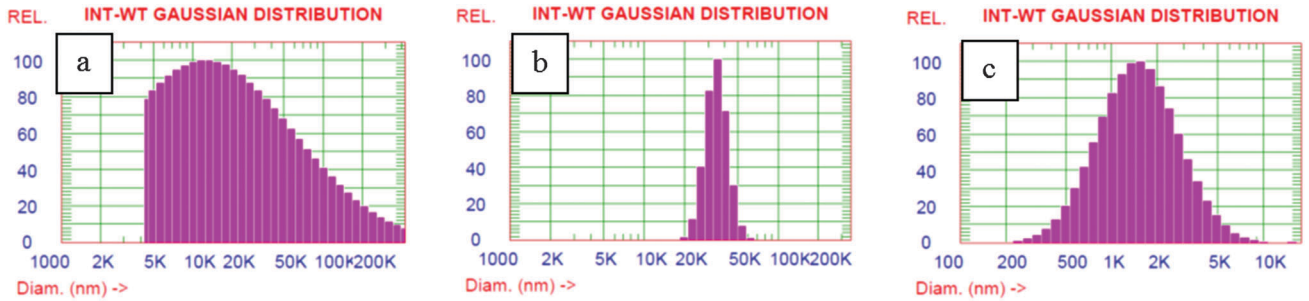

Fig. 7 Intensity weight averaged particle size distribution of stilbene (**1**) in (a) CTAB, (b) SDS and (c) Triton X-100. The sample concentration is of the order $\sim 2 \times 10^{-5}$ M at the surfactant concentrations above CMC values.

dye aggregates is polydisperse in the case of CTAB and Triton-X 100, while relatively sharp aggregates are noted for SDS. The overall size obtained from DLS measurements is due to aggregates in their hydrodynamic sphere and the interaction of surfactants seems to have a differential effect on the size of the hydrodynamic sphere of aggregates.

In order to understand whether the size of aggregates obtained in DLS corresponds solely to the probe or the surfactants, we carried out control experiments with surfactants alone. We attempted to record the aggregation sizes of the surfactants at above and below the CMC. We were successful in recording the particle size of the surfactants as they are mostly homogeneous solutions. Therefore, it is presumed that the sizes of aggregates obtained for the dye in surfactant solutions are solely because of the dye aggregates. Also to learn more about the interaction of stilbene with the surfactant assemblies, we have recorded fluorescence decay profiles. In water, a mono-exponential decay with a lifetime of 1.40 ns was observed. However, it exhibits bi-exponential decay in surfactant media below their CMC. This bi-exponential decay indicates a preferential location due to the interaction of stilbene (**1**) with the surfactant molecules. However, the data could not be fitted for either mono-exponential or poly-exponential for the decay profile for (**1**) at higher surfactant concentrations. The decay profiles and lifetime data are given in the ESI† (Fig. S7 and Table S2).

Conclusions

In summary, α-cyanostilbene (**1**) with unique aggregation induced enhanced emission properties was utilized as a fluorescence probe for determining critical micelle concentrations of anionic, cationic and neutral surfactants. Clear emission wavelength shifts with the concentration of the surfactant reveal aggregation induced enhanced emission shifts. The high sensitivity of this fluorophore can also be gauged by visible dual-color demarcation. Scanning electron microscopy images substantiate the formation of aggregates and morphological differences are noted at higher and lower surfactant concentrations.

Acknowledgements

The financial grant from the Department of Science and Technology, India, and support from IIT Gandhinagar are greatly appreciated. Help from IISER Kolkata in recording the single crystal data is appreciated. Thanks are also due to Dr Virupakshi Soppina for the help in fluorescence microscopy experiments and Dr Super Mishra for useful discussions.

References

1 Y. Hong, J. W. Y. Lam and B. Z. Tang, *Chem. Commun.*, 2009, 4332–4353.
2 D. Ding, K. Li, B. Liu and B. Z. Tang, *Acc. Chem. Res.*, 2013, **46**, 2441–2453.
3 Y. Yu, C. Feng, Y. Hong, J. Liu, S. Chen, K. M. Ng, K. Q. Luo and B. Z. Tang, *Adv. Mater.*, 2011, **23**, 3298–3302.
4 J. Mei, Y. Hong, J. W. Y. Lam, A. Qin, Y. Tang and B. Z. Tang, *Adv. Mater.*, 2014, **26**, 5429–5479.
5 H. J. Tracy, J. L. Mullin, W. T. Klooster, J. A. Martin, J. Haug, S. Wallace, I. Rudloe and K. Watts, *Inorg. Chem.*, 2005, **44**, 2003–2011.
6 J. Huang, X. Yang, J. Wang, C. Zhong, L. Wang, J. Qin and Z. Li, *J. Mater. Chem.*, 2012, **22**, 2478–2484.
7 N. B. Shustova, B. D. McCarthy and M. Dincă, *J. Am. Chem. Soc.*, 2011, **133**, 20126–20129.
8 B. Xu, Z. Chi, H. Li, X. Zhang, X. Li, S. Liu, Y. Zhang and J. Xu, *J. Phys. Chem. C*, 2011, **115**, 17574–17581.
9 J. He, B. Xu, F. Chen, H. Xia, K. Li, L. Ye and W. Tian, *J. Phys. Chem. C*, 2009, **113**, 9892–9899.
10 Z. Xie, B. Yang, G. Cheng, L. Liu, F. He, F. Shen, Y. Ma and S. Liu, *Chem. Mater.*, 2005, **17**, 1287–1289.
11 J. Gierschner, L. Lüer, B. Milián-Medina, D. Oelkrug and H.-J. Egelhaaf, *J. Phys. Chem. Lett.*, 2013, **4**, 2686–2697.
12 B.-K. An, D.-S. Lee, J.-S. Lee, Y.-S. Park, H.-S. Song and S. Y. Park, *J. Am. Chem. Soc.*, 2004, **126**, 10232–10233.
13 K. A. N. Upamali, L. A. Estrada, P. K. De, X. Cai, J. A. Krause and D. C. Neckers, *Langmuir*, 2011, **27**, 1573–1580.
14 Y. Liu, M. Kong, Q. Zhang, Z. Zhang, H. Zhou, S. Zhang, S. Li, J. Wu and Y. Tian, *J. Mater. Chem. B*, 2014, **2**, 5430–5440.
15 S. Kaur, A. Gupta, V. Bhalla and M. Kumar, *J. Mater. Chem. C*, 2014, **2**, 7356–7363.
16 R. Chopra, P. Kaur and K. Singh, *Anal. Chim. Acta*, 2015, **864**, 55–63.
17 B.-K. An, S.-K. Kwon, S.-D. Jung and S. Y. Park, *J. Am. Chem. Soc.*, 2002, **124**, 14410–14415.

18 N.-W. Tseng, J. Liu, J. C. Y. Ng, J. W. Y. Lam, H. H. Y. Sung, I. D. Williams and B. Z. Tang, *Chem. Sci.*, 2012, **3**, 493–497.
19 Y. Hong, J. W. Y. Lam and B. Z. Tang, *Chem. Soc. Rev.*, 2011, **40**, 5361–5388.
20 B.-R. Gao, H.-Y. Wang, Y.-W. Hao, L.-M. Fu, H.-H. Fang, Y. Jiang, L. Wang, Q.-D. Chen, H. Xia, L.-Y. Pan, Y.-G. Ma and H.-B. Sun, *J. Phys. Chem. B*, 2009, **114**, 128–134.
21 L. Wang, L. Yang and D. Cao, *Curr. Org. Chem.*, 2014, **18**, 1028–1049.
22 Y. Zhang, D. Li, Y. Li and J. Yu, *Chem. Sci.*, 2014, **5**, 2710–2716.
23 Y.-D. Lee, C.-K. Lim, A. Singh, J. Koh, J. Kim, I. C. Kwon and S. Kim, *ACS Nano*, 2012, **6**, 6759–6766.
24 R. Zhang, Y. Yuan, J. Liang, R. T. K. Kwok, Q. Zhu, G. Feng, J. Geng, B. Z. Tang and B. Liu, *ACS Appl. Mater. Interfaces*, 2014, **6**, 14302–14310.
25 D. Wang, J. Qian, W. Qin, A. Qin, B. Z. Tang and S. He, *Sci. Rep.*, 2014, **4**, 4279.
26 V. Palakollu and S. Kanvah, *New J. Chem.*, 2014, **38**, 5736–5746.
27 O. V. Dolomanov, L. J. Bourhis, R. J. Gildea, J. A. K. Howard and H. Puschmann, *J. Appl. Crystallogr.*, 2009, **42**, 339–341.
28 L. Palatinus and G. Chapuis, *J. Appl. Crystallogr.*, 2007, **40**, 786–790.
29 L. J. Farrugia, *J. Appl. Crystallogr.*, 2012, **45**, 849–854.
30 C. B. Hubschle, G. M. Sheldrick and B. Dittrich, *J. Appl. Crystallogr.*, 2011, **44**, 1281–1284.
31 C. F. Macrae, I. J. Bruno, J. A. Chisholm, P. R. Edgington, P. McCabe, E. Pidcock, L. Rodriguez-Monge, R. Taylor, J. van de Streek and P. A. Wood, *J. Appl. Crystallogr.*, 2008, **41**, 466–470.
32 M. Nardelli, *J. Appl. Crystallogr.*, 1995, **28**, 659.
33 A. Spek, *Acta Crystallogr., Sect. D: Biol. Crystallogr.*, 2009, **65**, 148–155.
34 C. F. Macrae, I. J. Bruno, J. A. Chisholm, P. R. Edgington, P. McCabe, E. Pidcock, L. Rodriguez-Monge, R. Taylor, J. v. Streek and P. A. Wood, *J. Appl. Crystallogr.*, 2008, **41**, 466–470.
35 C. A. Bunton, F. Nome, F. H. Quina and L. S. Romsted, *Acc. Chem. Res.*, 1991, **24**, 357–364.
36 M. Pérez-Rodríguez, G. Prieto, C. Rega, L. M. Varela, F. Sarmiento and V. Mosquera, *Langmuir*, 1998, **14**, 4422–4426.
37 A. Dominguez, A. Fernandez, N. Gonzalez, E. Iglesias and L. Montenegro, *J. Chem. Educ.*, 1997, **74**, 1227.
38 X. Cai, W. Yang, L. Huang, Q. Zhu and S. Liu, *Sens. Actuators, B*, 2015, **219**, 251–260.
39 P. Mukerjee and K. J. Mysels, *Natl. Std. Ref. Data Ser National Bureau of Standards*, Washington DC, 1971.